

physica **p** status **s** solidi **S**

www.interscience.wiley.com

reprints

physica status solidi ^a
www.pss-a.com
applications and materials science
Editor's Choice
Highly efficient all-nitride phosphor-converted white light emitting diode
(Regina Mueller-Mach et al., p. 1727)
WILEY-VCH
www.pss-a.com

physica status solidi ^b
www.pss-b.com
basic solid state physics
Current Trends in Electronic Structure: Embedding and Linear Scaling Techniques
Thomas Beck, and Eduardo Hernandez
SPECIAL ISSUE
www.pss-b.com

physica status solidi ^c
[www.pss-c.com
current topics in solid state physics
Resonance feedback color center lasers in wide band gap materials excited by a pair of chirped femtosecond pulses
\(Kobori et al., p. 637\)
\[www.pss-c.com\]\(http://www.pss-c.com\)](http://www.pss-c.com)

physica status solidi ^r
www.pss-rapid.com
rapid research letters
www.pss-rapid.com

Effect of the deposition rate on ITO thin film properties prepared by ion beam assisted deposition (IBAD) technique

Li-Jian Meng^{*1,2}, V. Teixeira², and M. P. dos Santos^{3,4}

¹Departamento de Física, Instituto Superior de Engenharia do Porto, Rua Dr. António Bernardino de Almeida, 431, 4200-072 Porto, Portugal

²Centro de Física, Universidade do Minho, 4800-058 Guimarães, Portugal

³CeFITec, Universidade Nova de Lisboa, Lisboa, Portugal

⁴Departamento de Física, Universidade de Évora, Évora, Portugal

Received 20 May 2009, revised 15 January 2010, accepted 18 January 2010

Published online 2 June 2010

Keywords electrical properties, ion-assisted deposition structure, ITO, optical properties

* Corresponding author: e-mail ljm@isep.ipp.pt, Phone: +00 351 962 325 429, Fax: +00 351 228 321 159

Indium tin oxide (ITO) thin films have been deposited onto glass substrates at room temperature by ion beam assisted deposition technique at different deposition rates (0.1–0.3 nm/s). The effects of the deposition rate on the structural, optical and electrical properties of the deposited films have been studied. The optical constants of the deposited films were calculated by fitting the transmittance spectra using the semi-

quantum model. Considering the application for the electromagnetic wave shielding which needs a high IR reflectance, the optimising deposition rate is 0.2 nm/s. The films prepared at this deposition rate shows a relative high IR reflectance (60%), a good electrical conductivity ($5 \times 10^{-3} \Omega \text{ cm}$), and a reasonable transmittance in the visible region (over 80%).

© 2010 WILEY-VCH Verlag GmbH & Co. KGaA, Weinheim

1 Introduction Indium tin oxide (ITO) film is a wide band gap semiconductor and has been widely used in many electronics and optoelectronics applications, such as flat panel displays, organic light emitting diodes (OLED) and solar cells, because of its high transmittance in the visible region and high electrical conductivity [1–3]. In addition, its high infrared reflection has also found the applications in thermal insulation of windows and in some electromagnetic wave shielding [4, 5]. ITO film also exhibits its excellent substrate adherence, hardness and chemical stability. Due to these excellent properties of ITO films, the study on it has never been interrupted.

Many physical and chemical deposition techniques have been used for fabricating the ITO films, such as various evaporation and sputtering techniques, and several chemical vapour deposition techniques. Generally, in order to get the ITO films with high transmittance and good electrical conductivity using these deposition techniques, the substrate needs to be heated during the deposition process, or post-deposition annealing is needed [6, 7]. Recently, there is a

growing interest in applying organic substrates for liquid crystal display devices and light emitting diodes as they are lighter and thinner than glass substrates. As the organic substrates cannot withstand the high temperature, preparing the ITO films at low temperature, particularly at room temperature, is full of challenge.

Although sputtering and reactive evaporation technique can produce ITO films with low electrical resistivity, the oxygen gas flow during the deposition processes needs to be controlled very precisely. Some small variations on oxygen flow will result in a big different on ITO films properties. It has been found that the ion beam assisted deposition (IBAD) technique is a suitable technique for low temperature deposition. By using this deposition technique, one gets more flexibility in controlling film properties and the ITO films prepared at room temperature without any post-deposition annealing has a high transmittance and good electrical conductivity. It is also a low cost production technique [8–11]. In this work, the physical properties of ITO films prepared at different deposition rates by IBAD technique have been studied.

Table 1 Deposition conditions and some properties of ITO films prepared at different deposition rates.

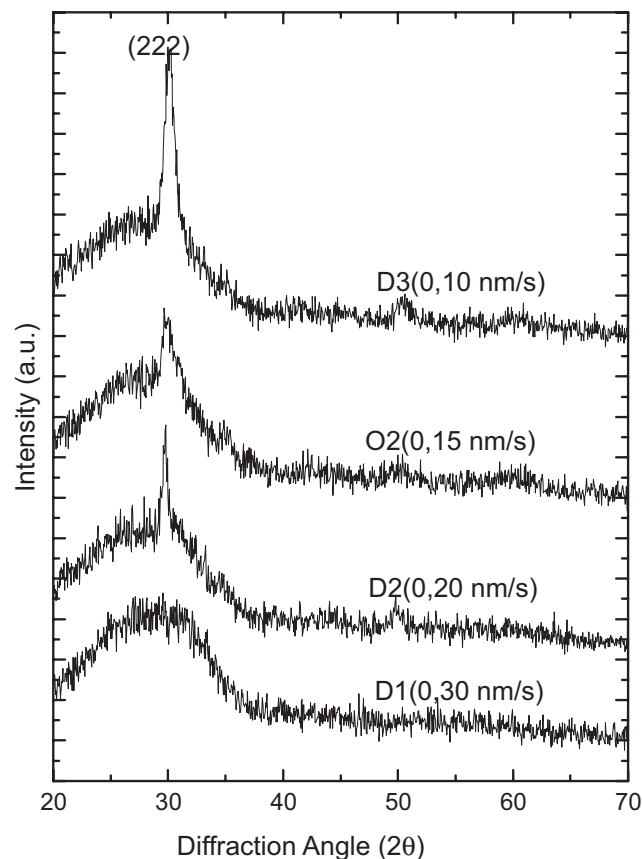
sample	D1	D2	O2	D3
deposition rate (nm/s)	0.3	0.2	0.15	0.1
deposition time (s)	718	1 033	1 353	2 004
thickness (nm)	230	215	228	224
sheet resistance (Ω /square)	323	51	94	1.4×10^6
resistivity ($10^{-3} \Omega \text{ cm}$)	34	5	10	1.4×10^5
carrier concentration (10^{20} cm^{-3})	1.3	2.7	0.8	1.9×10^{-3}
Hall mobility ($\text{cm}^2/\text{V s}$)	7	21	37	1
surface roughness by AFM (nm)	2.5	1.4	0.3	1.2
<i>d</i> -spacing between (222) planes (nm) (standard value $d_0 = 0.2923 \text{ nm}$)		0.3039	0.2973	0.2967
grain size along (222) direction (nm)		16	6	8
measured IR reflectance at 12 000 nm	37%	63%	45%	20%
calculated IR reflectance	14%	62%	45%	0%

2 Experimental details ITO films were deposited onto commercial k9 glass substrates at room temperature by IBAD technique using a vacuum coater equipped with two electron beam guns (only one of them was used in this work) and a Kaufman ion source. ITO powder pellet with a composition of 90 wt.% In_2O_3 and 10 wt.% SnO_2 was used as the evaporation source material. A 120 mm diameter Kaufman ion source was used to generate oxygen ion beam. The oxygen gas flow was controlled by a mass flow controller. The deposition rate and the film thickness were monitored and controlled by a quartz crystal sensor which has been linked to e-beam power supply for automatic controlling. The nominal deposition rate was set to be 0.1, 0.15, 0.2 and 0.3 nm/s, respectively. The thickness was preset at 200 nm. The film thickness indicated in Table 1 was obtained by fitting the transmittance spectra. The substrate holder was rotated at a speed of 0.3 rounds/s. The angle between the incident oxygen ion beam and the normal of the substrate holder was fixed at 45° . Before the deposition, the chamber was evacuated until a pressure of $1 \times 10^{-3} \text{ Pa}$. After that, the oxygen gas was introduced into the chamber. The oxygen flow was set to be 40 sccm, and the dynamic pressure in the chamber was about $2.3 \times 10^{-2} \text{ Pa}$. During all depositions, the ion beam current, the accelerating voltage and the screen voltage were kept constants at 100 mA, 250 and 500 V, respectively.

The optical transmittance spectra of the films were recorded by Perkin-Elmer Lambda 900 UV/VIS/NIR spectrometer and the infrared reflectance was measured by Perkin-Elmer Spectrum GX at angle of incidence of 60° related to the substrate normal. Atomic force microscopy (AFM) measurements were made using the equipment from Digital Instruments Veeco Metrology Group. The X-ray diffraction was done by SHIMADZU XRD-6000 performed between the 2θ values of $20 \sim 70^\circ$ with a step of 0.05° . The Hall effect was measured using Lake Shore 665 with a 5 kG magnetic field intensity at room temperature. All the experimental error depends on the respective measuring equipments.

3 Results and discussion X-ray diffraction patterns of the ITO films show that the films prepared at the deposition rate lower than 0.2 nm/s have a cubic In_2O_3

structure [12] with a preferred orientation along the (222) direction. As exhibited in Fig. 1, the film deposited at high deposition rate (higher than 0.3 nm/s) shows an amorphous structure. Although the ITO powder pellet with a composition of 90 wt.% In_2O_3 and 10 wt.% SnO_2 was used as the evaporation source material, during the evaporation, the oxygen may get lost. As the deposition rate is increased, the e-beam power must be increased. That may result in more lost of the oxygen. It means more oxygen must be introduced

**Figure 1** XRD patterns of the ITO films deposited at different deposition rates.

into the chamber to compensate the lost. As we kept the oxygen flow constant for all the deposition rates, it may not be enough to form the polycrystalline ITO films at high deposition rate and result in an amorphous structure. The distance between the (222) crystal planes has been calculated and the crystalline dimension along the (222) direction has been estimated using Scherrer formula [13] by fitting the X-ray diffraction peak. The results are given in Table 1. It has been found that the distance between the (222) crystal planes for all the polycrystalline ITO films are higher than the standard stress-free value (0.2923 nm) [12], and the difference becomes big as the deposition rate is increased. It means that there are compressive stresses in all the polycrystalline films and the stress value is increased as the deposition rate is increased. Although the ITO film deposited at 0.2 nm/s is subject to a big compressive stress, it has a big crystalline size.

The surface morphology of the ITO films deposited at different deposition rates was studied by AFM in a non-contact mode as shown in Fig. 2. The surface roughness [root mean square (rms) value] has been calculated for the different ITO films and is listed in Table 1. The ITO film

prepared at 0.15 nm/s has a smooth surface and the ITO film prepared at 0.3 nm/s has a rough surface. Generally, crystalline film has the rough surface [14]. However, our amorphous ITO film shows a rough surface comparing to the crystalline films. At the high deposition rate, there is not enough oxygen to form stoichiometric ITO film and metal rich ITO film may be formed and results in a rough surface.

Figure 3 shows the specular transmittance spectra of the ITO films prepared at different deposition rates. It can be seen that the transmittance decreases as the deposition rate is increased. As we kept oxygen flow constant for all the deposition rates, the ITO films deposited at high deposition rate can not be fully oxidized and result in a decrease of the transmittance. It can be seen that the transmittance of the ITO films show a big decrease when the deposition rate is higher than 0.2 nm/s. It means the deposition rate must be kept below the 0.2 nm/s in order to get ITO films with good optical properties.

In order to calculate the optical constant of the ITO films, the transmittance (between 400 and 1800 nm) have been fitted using semi-quantum model [15, 16] combined with

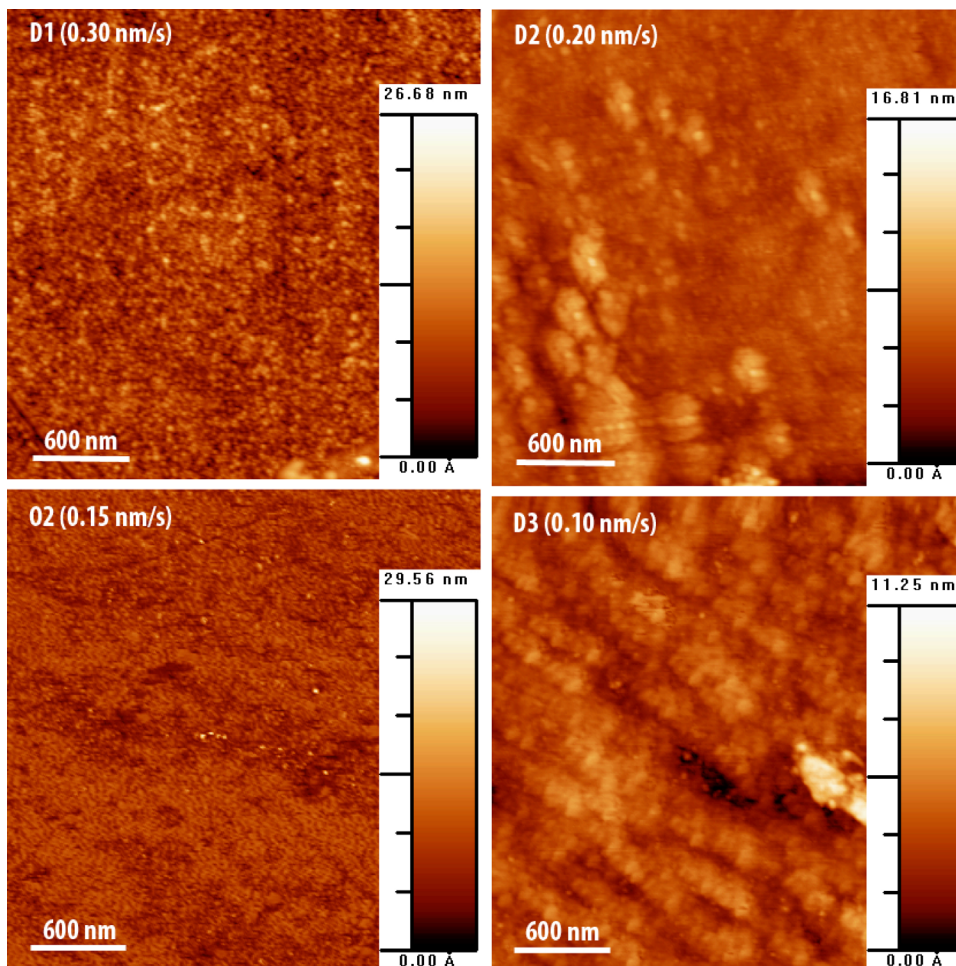


Figure 2 (online colour at: www.pss-a.com) AFM images ($3\ \mu\text{m} \times 3\ \mu\text{m}$) of the surface of the ITO films deposited at different deposition rates.

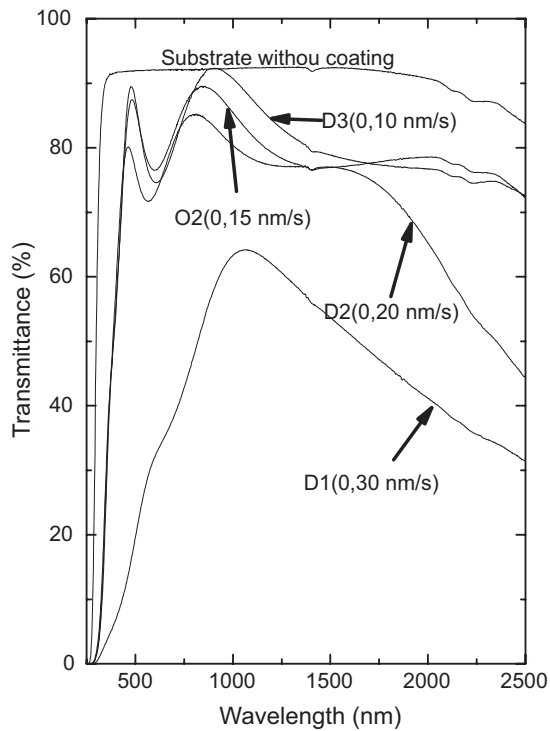


Figure 3 Specular transmittance as a function of the wavelength for the ITO films deposited at different deposition rates.

Drude model. The dielectric function can be described as follows:

$$\varepsilon(\omega) = \varepsilon_{\infty} \prod_j \frac{\omega_{jLO}^2 - \omega^2 - i\gamma_{jLO}\omega}{\omega_{jTO}^2 - \omega^2 - i\gamma_{jTO}\omega} + \frac{\omega_p^2}{-\omega^2 + i\gamma_d\omega} \quad (1)$$

The first term is the semi-quantum model and it represents the dielectric function as a product of individual oscillator terms. For each term there are four parameters, where ω_{jTO} , γ_{jTO} , ω_{jLO} and γ_{jLO} are the resonance frequencies and damping constants of the transverse and longitudinal optical modes, respectively. ε_{∞} is the 'high-frequency' contribution to the dielectric function. The second term is the Drude model contribution which is used to modify the free electron properties. Very good fits have been obtained for all the ITO films using these models. The fitting parameters are listed in Table 2.

After fitting, the refractive index and extinction coefficient can be obtained as shown in Fig. 4. It can be seen that the extinction coefficient for ITO films increases as the deposition rate is increased. It has been seen from Fig. 3 that as the deposition rate is increased, the transmittance of the ITO films decreases and then results in an increase of the extinction coefficient. The refractive index of the ITO films deposited at low (0.1 nm/s) and high (0.3 nm/s) deposition rate have high refractive index. At the low deposition rate, the 40 sccm oxygen flow is enough to oxidize deposited film

Table 2 Fitting parameters.

sample	D1	D2	O2	D3
ε_{∞}	0.20	3.69	3.33	4.23
ω_p (cm ⁻¹)	474	10 110	7 195	4 895
γ_d (cm ⁻¹)	1 00 000	528	731	853
ω_{LO1} (cm ⁻¹)	2 58 520	6 654	7 200	5 783
γ_{LO1} (cm ⁻¹)	2 00 000	4 758	5 069	3 672
ω_{TO1} (cm ⁻¹)	320	6 584	7 132	5 774
γ_{TO1} (cm ⁻¹)	47 787	4 653	5 052	3 760
ω_{LO2} (cm ⁻¹)	4 504	35 861	36 809	25 286
γ_{LO2} (cm ⁻¹)	3 378	6 650	9 974	5 174
ω_{TO2} (cm ⁻¹)	14 514	33 593	33 651	25 148
γ_{TO2} (cm ⁻¹)	52 428	5 750	7 731	5 088
discrepancy	0.005	0.005	0.005	0.005

and forms the stoichiometric ITO film. The stoichiometric ITO film has a high packing density and a high refractive index. As the deposition rate is increased, the same oxygen flow is not enough to fully oxidize deposited ITO films and results in more oxygen vacancies in the deposited films and then reduce the packing density and show a low refractive index. When the deposition rate reaches to 0.3 nm/s, the deposited films structure changed as shown in Fig. 1 and may result in the high refractive index. The thickness of the deposited ITO films is also obtained by fitting the transmittance. The results are listed in Table 1. All the films show a similar thickness about 220 nm and are little bit higher than the predefined value (200 nm).

The electrical properties of the deposited ITO films are listed in Table 1. The ITO film deposited at low deposition

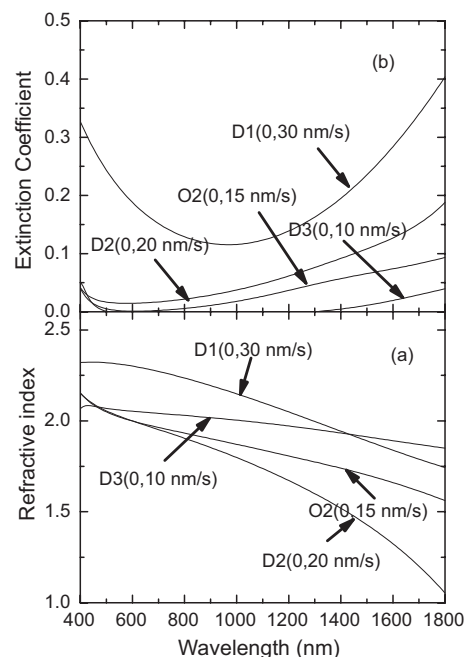


Figure 4 Refractive index (a) and extinction coefficient (b) as a function of the wavelength for the ITO films deposited at different deposition rates.

rate (0.1 nm/s) has very low electron concentration and then a very high electrical resistivity. At low deposition rate, deposited ITO films are fully oxidized and only a few oxygen vacancies exist and result in a low electron concentration. As the deposition rate is increased, the deposited ITO films cannot be fully oxidized and more oxygen vacancies are formed and produce more electrons. From Table 1 it can be seen that the films deposited at 0.15–0.2 nm/s deposition rates have high Hall mobility, high electron concentration and low electrical resistivity.

Figure 5 shows the reflectance FTIR spectra for ITO films prepared at different deposition rates. The spectra shown were obtained for angles of incidence of 60° related to the substrate normal. It can be seen from the figure that the reflectance increases as the deposition rate is increased from 0.1 to 0.2 nm/s. When the deposition rate is increased further, the reflectance decreases. There is a very simple relation between the infrared reflection R and the sheet resistance R_{sr} [17, 18]:

$$R_{IR} = (1 + 2\varepsilon_0 c_0 R_{sr})^{-2}. \quad (2)$$

The reflectance of ITO films deposited at different deposition rates has been calculated by this equation. The results are listed in Table 1, and to compare, the measured reflectances at 12 000 nm are also listed in the Table. It can be seen that only for the sample prepared at 0.15–0.2 nm/s deposition rates, the calculated value is in good accordance

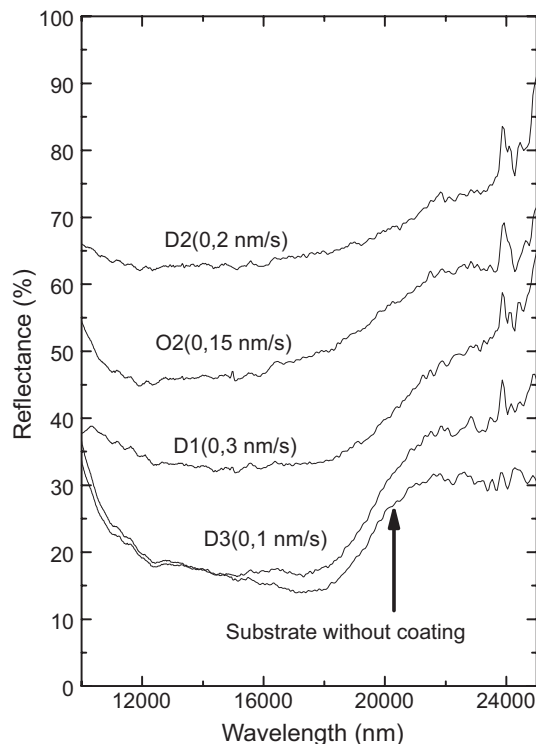


Figure 5 Infrared reflectance spectra for ITO films deposited at different deposition rates.

with the measured value. It means this equation can only give good results for samples with low sheet resistance.

4 Conclusions ITO films have been deposited onto glass substrates at different deposition rates by IBAD technique. During all the deposition processes, the oxygen flow is kept constant at 40 sccm and the deposition rate is varied from 0.1 to 0.3 nm/s. The films deposited at low deposition rate (lower than 0.2 nm/s) show polycrystalline structure and give a preferred orientation along the (222) direction. The films prepared at high deposition rates (higher than 0.3 nm/s) show an amorphous structure. All the polycrystalline structure ITO films are subject to a compressive residual stress and as the deposition rate increases, the residual stress increases. The film deposited at high deposition rate leads to a high surface roughness.

The films prepared at low deposition rate (0.1 nm/s) show high optical transmittance. As the deposition rate increases, transmittance is decreased. The films deposited at the deposition rate of 0.15–0.2 nm/s exhibit good electrical properties ($5\text{--}10 \times 10^{-3} \Omega \text{cm}$). Considering both the optical and electrical parameters, the deposition rate should be kept between 0.15 and 0.2 nm/s. The ITO films deposited at 0.2 nm/s deposition rate gives high IR reflectance which is very useful for some electromagnetic wave shielding applications.

References

- [1] I. Hamberg and C. G. Granqvist, *J. Appl. Phys.* **60**(11), R123 (1986).
- [2] S. H. Choi, J. T. Kim, C. S. Kim, and H. K. Baik, *Appl. Phys. Lett.* **90**, 033513 (2007).
- [3] S. K. Park, J. I. Han, W. K. Kim, and M. G. Kwak, *Thin Solid Films* **397**, 49 (2001).
- [4] L. Yang, X. He, and F. He, *Mater. Lett.* **62**(30), 4539 (2008).
- [5] J. L. Huang, B. S. Yau, C. Y. Chen, W. T. Lo, and D. F. Lii, *Ceram. Int.* **27**, 363 (2001).
- [6] L. J. Meng, A. Maçarico, and R. Martins, *Vacuum* **46**, 673 (1995).
- [7] P. Canhola, N. Martins, L. Raneiro, S. Pereira, E. Fortunato, I. Ferreira, and R. Martins, *Thin Solid Films* **487**, 271 (2005).
- [8] D. Kim and S. Kim, *Thin Solid Films* **408**, 218 (2002).
- [9] C. Liu, T. Mihara, T. Matsutani, T. Asanuma, and M. Kiuchi, *Solid State Commun.* **126**, 509 (2003).
- [10] P. J. Martin, R. P. Neterfield, and D. R. McKenzie, *Thin Solid Films* **137**, 207 (1986).
- [11] M. Gilo, R. Dahan, and N. Croitoru, *Opt. Eng.* **38**, 953 (1999).
- [12] Powder Diffraction File, Joint Committee on Powder Diffraction Standards, 1967 (ASTM, Philadelphia, PA, 1967) Card 6-0416.
- [13] B. D. Cullity, *Elements of X-ray Diffraction*, 2nd ed. (Addison-Wesley, Reading, MA, 1978).
- [14] H. Kim, J. S. Horwitz, G. Kushto, A. Piqué, Z. H. Kafafi, C. M. Gilmore, and D. B. Chrisey, *J. Appl. Phys.* **88**, 6021 (2000).
- [15] F. Gervais and B. Piriou, *Phys. Rev. B* **11**, 3944 (1975).
- [16] M. Schubert, T. E. Tiwald, and C. M. Herzinger, *Phys. Rev. B* **61**, 8187 (2000).
- [17] P. K. Biswas, A. De, N. C. Pramanik, P. K. Chakraborty, K. Ortner, V. Hock, and S. Korder, *Mater. Lett.* **57**, 2326 (2003).
- [18] G. Frank, E. Kauer, and H. Kostlin, *Thin Solid Films* **77**, 107 (1981).